UCRL-JC-123553

CONF-9606116--76

Modeling and Experiments of X-Ray Ablation of National Ignition Facility First Wall Materials

A. T. Anderson, A. K. Burnham,
M. T. Tobin, and P. F. Peterson

This paper was prepared for submittal to the
American Nuclear Society 12th Topical Meeting on the
Technology of Fusion Energy
Reno, NV
June 16-20, 1996

June 4, 1996

Lawrence Livermore National Laboratory

DISCLAIMER

Modeling and Experiments of X-Ray Ablation of National Ignition Facility First Wall Materials

Andrew T. Anderson
LLNL
P.O. Box 808
Livermore, CA 94551
(510) 423-9634

Alan K. Burnham
LLNL
P.O. Box 808
Livermore, CA 94551
(510) 422-7304

Michael T. Tobin
LLNL
P.O. Box 808
Livermore, CA 94551
(510) 423-1168

Per F. Peterson
U. C. Berkeley
4111 Etchevery Hall
Berkeley, CA 94720
(510) 643-7749

ABSTRACT

This paper discusses results of modeling and experiments on the x-ray response of selected materials relevant to the NIF target chamber design. X-ray energy deposition occurs in such small characteristic depths (on the order of a micron) that thermal conduction and hydrodynamic motion significantly affect the material response, even during the typical 10-ns pulses. The finite-difference ablation model integrates four separate processes: x-ray energy deposition, heat conduction, hydrodynamics, and surface vaporization.

Experiments have been conducted at the Nova laser facility in Livermore on the response of various materials to NIF-relevant x-ray fluences. Samples of fused silica, silicon nitride, boron carbide, boron, silicon carbide, carbon, aluminum oxide, and aluminum were tested. The response was diagnosed using post-shot examinations of the surfaces with scanning electron microscope (SEM) and atomic force microscope (AFM) instruments. On the basis of these observations, judgments were made about the dominant removal mechanisms for each material. The relative importances of these processes were also investigated with the x-ray response model.

I. INTRODUCTION

Ablation of material from the National Ignition Facility (NIF) chamber wall is a major threat to the laser final optics. Wall material condensing on these optics after a shot may cause damage with subsequent laser shots. For this reason, the aluminum chamber walls of the NIF chamber will be protected with panels of refractory material. This first wall material, at 5 m from the target, may receive a peak x-ray fluence from a 20-MJ yield shot of about 2.5 J/cm^2, released over a few to a few tens of nanoseconds. This x-ray threat is sufficiently potent that some material may be ablated from the first wall surface. Removal rates must be predicted accurately to ensure the successful operation of the target chamber.

The goal for this effort is to produce a validated material x-ray response model for NIF first wall response. The first step is to develop models based on current knowledge of material removal processes. The second step is to conduct experiments both to provide benchmark data for the models and to identify removal mechanisms for specific materials to further guide the modeling work. The third step is to develop and refine the models to match the experimental data. Finally the validated models can be applied to NIF x-ray conditions to accurately predict material response.

II. MODELING

A. Overview

The transient ablation modeling has two goals. The first is to predict the amount of material removed by the x rays (the ablation depth). The second goal is to determine the state of the ablated material after it leaves the surface. This includes information on velocity and temperature and whether the material is liquid drops or vapor. Of primary importance are the total amount and form of any material in the chamber that may deposit on the optics and cause damage during subsequent shots.

To accomplish these goals, four processes are included in the finite-difference ablation model developed here (a code called ABLATOR). The first process is the energy deposition from the x rays through the thin surface layers of material. A transient thermal conduction model allows this energy to move between zones, which is particularly important near the strongly heated surface layer. Heating causes thermal expansion, which raises pressures and causes hydrodynamic motion as the pressures release from the surface. The fourth part of the model describes the removal of material through kinetically-limited surface vaporization.

B. X-ray Deposition Model

X rays of a particular photon energy deposit according to a simple exponential attenuation. This uses cross-sections based on the cold opacity of the material for x rays at that energy. The photon energy range from 1 eV to 20 keV is divided into 45 bins, each of which is treated as a monoenergetic deposition process. A sensitivity study indicated that this group structure gives a fairly accurate representation of the steps and edges in the typical opacity curves, and so of the energy deposition. Energy is deposited into the Lagrangian zones in each time step according to the given x-ray energy pulse shape. The total energy added at any depth is the sum over all energy groups.

C. Heat Conduction Model

In the code, energy conservation is based on directly tracking the internal energy of each Lagrangian zone. This avoids some of the difficulties encountered in temperature and heat capacity based methods near phase change boundaries. Temperature is specified for each phase (solid, liquid, and vapor) as a function of enthalpy. The temperature is used in two ways. Primarily, it is used to calculate the net thermal conduction for each time step according to a simple explicit Fourier model. It is also used in empirical correlations of thermal conductivity with temperature.

D. Mechanical Response Model

A finite-difference hydrodynamic model was implemented to track stress wave and material motion caused by the sudden energy deposition. The algorithms are based on those of the WONDY code[1]. At each time step, the zone energy and density information, combined with an equation of state (EOS), give the pressure and stress in each zone. The EOS forms are typically Gruneisen for solid / liquid and ideal gas for vapor. The stresses are used to compute accelerations with F=ma, which in turn gives new velocities and zone boundary locations. With the (constant) zone mass, densities can be determined to continue the cycle.

E. Surface Vaporization Model

Vaporization is assumed to occur only at the free surface. The rate of evaporation is governed by the maximum flux of atoms per unit area that would occur under equilibrium vapor/liquid conditions. The resulting flux, given by

$$\text{Flux} = P_{sat} * (2\pi mkT)^{(-1/2)} \quad (1)$$

increases exponentially with surface temperature, through the saturation pressure term. Therefore for kinetically-limited evaporation, no single "boiling temperature" exists and vaporization occurs continuously over a range of temperatures, typically several thousand degrees Centigrade. This mass flux is an upper limit, in that no recondensation is included. This approximation is reasonable for exposures in the Nova and NIF target chambers, which are under vacuum.

The treatment of x-ray ablation in ABLATOR differs from those found in several computer codes relevant to ICF chamber design, including CONRAD[2] (now BUCKY) from the University of Wisconsin, TSUNAMI[3] from UC Berkeley, and the codes used by SRI Intl. (FSCATT, SRI PUFF)[4]. These models determine x-ray vaporization depths from energy distribution profiles based on instantaneous deposition. The vaporized depth is typically taken as the point in the energy profile where the cohesive or sublimation energy is exceeded. Such models do not account for the limitations in surface vapor flux, but may be adequate in strongly heated systems, where super-critical conditions allow very hot "fluid" to leave the bulk material without a distinct phase change.

III. EXPERIMENTS

A. Introduction

Ablation experiments are the second step in the process of developing a validated material x-ray response model. One goal of these tests is to determine removal mechanisms for various materials. This guides the modeling efforts to predict removal under given conditions. For the tested materials, the modeling is then a direct means of extrapolating to their response to conditions in other ICF facilities. For materials not examined in these tests, predictions can be made with this model for removal mechanisms and ablation depths based on the material properties. The second goal of the experiments is to provide quantitative data on ablation depths to benchmark the performance of the models.

Eight different materials were examined in this series of experiments. Boron carbide and boron are prime candidates for the NIF first wall coating. Silicon carbide, carbon, silicon nitride, and aluminum oxide are other possibilities. Fused silica is planned to cover about 10% of the first wall surface area in its role as a beam dump cover. Aluminum is a typical structural material in the chamber system, so its x-ray response is also significant.

B. Experiment Description

The material ablation studies were conducted over the course of 27 separate laser shots on Nova. On each of these shots, ten or eleven material samples were exposed at various stand-off distances to x rays generated in a target hohlraum. Because many samples received multiple exposures, the total number of samples exposed was 67. Masking of the sample surfaces with thin tantalum foils provided several different exposure levels on each sample. The 1.25-cm diameter samples were placed at distances from 21 to 40 cm from the target, giving x-ray fluences ranging from 1.0 to 3.5 J/cm^2. The typical x-ray pulse was 1 - 2 ns long, with a spectrum approximating a 200-250 eV blackbody. Several sources of debris were present in these shots, including the hohlraum, shields, and target supports. But because the debris-affected regions were limited to a relatively small surface area, the debris was not a serious problem. These conditions give absolute fluences 1.5 to 2 times higher than those predicted for the NIF first wall, although the spectra and pulse lengths are different. Therefore these tests span a relevant range of conditions for benchmark tests and extrapolation to NIF chamber response.

All observations and measurements from this series of experiments are based on post-shot analyses of the exposed samples. Optical microscopy, combined with SEM and AFM images, provide the basis for conclusions on material removal mechanisms. Quantitative data on material removal depths was obtained by measuring surface height changes between regions exposed to different numbers of shots. A Tencor alpha-step 200 was the primary instrument used for this part of the analysis, supplemented in some cases by AFM data.

C. Material removal mechanisms

Several different removal mechanisms were identified during the course of experimentation. These are vaporization, thermal shock/spall, and liquid splash. This section discusses the general features of each mechanism, while the following sections detail which phenomena occur in specific materials.

X-ray energy deposition in the fluence range of interest produces high surface temperatures, on the order of several thousand degrees. Vaporization from these hot solid or liquid surfaces into the chamber vacuum is expected for nearly any material. However, the amount of vapor removal may or may not be significant, depending on the particular thermal and chemical response of a material. This is because the rate of evaporation varies exponentially with surface temperature, through the dependence on equilibrium vapor pressure. Materials that ablate primarily through vaporization (e.g., fused silica) show several common features in the post-shot examinations. The exposed surfaces are smooth and flat, not significantly worse than the original finish. The steps measured by profilometry are sharp and well defined. The ablation depths increase linearly with the number of exposures, for multiply exposed sample regions.

Thermal shock/spall is the second material removal mechanism noted in the experiments, most notably in the boron and boron carbide results. Damage starts when the melt layer generated after the x-ray exposure solidifies. This material will be in a stress-free state at an elevated temperature somewhat below the melt point. As it cools, the surface layer will be put under tension, because the underlying bulk material constrains any lateral motion. If the stresses exceed the tensile strength, brittle materials will develop thermal stress cracks on the surface. Subsequent x-ray exposures can remove damaged material in two ways. One cause is the shock and rarefaction waves generated by absorbing the x-ray pulse. The other mechanism is additional thermal stress upon cooling the already damaged material. Thermal stress cracks in the exposed surfaces are the obvious visual indications of materials susceptible to the thermal shock/spall process. The other clue is the presence of angular pits of a size consistent with the spall damage flakes.

The final removal mechanism is ejection of liquid from the exposed surface, easily seen in the aluminum exposures. For fluences above the damage threshold, a melt layer forms quickly during the x-ray pulse. The heating also causes thermal expansion, which accelerates the melted surface layer away from the bulk material. After the pulse ends, so does the rapid thermal expansion. The velocity of the surface layer then quickly drops to near zero as a result of tensile stresses from the bulk material. The deceleration of the liquid layer causes Rayleigh-Taylor instabilities that make the surface wavy and eventually release material in the form of droplets. The short pulse duration may not allow sufficient time for instability growth in a single shot. Some "conditioning shots" may therefore be required to alter the surface geometry before material is removed. Kelly[5] has noted a similar conditioning requirement for melt removal from metals exposed to laser pulses, although the mechanism is somewhat different.

Several observations are typical of materials subject to significant liquid removal. The surfaces tend to be wavy with well-rounded crests and valleys. Because of the lateral liquid motion, the surfaces are also very rough. Droplets are frequently observed, either resting on the surface or attached to a crest by a narrow neck of material. Near boundaries of regions with different numbers of x-ray exposures, splash in the form of droplets or thin fibers is also commonly seen.

D. Summary of observations

Post-shot analyses of exposed material samples included optical microscopy, SEM, AFM, and profilometry. With these tools, the characteristics of ablation for each of the materials were determined. Table 1 presents our findings and relates these observations to likely removal mechanisms.

Table 1: Summary of material removal observations and ablation mechanisms.

Material	Observations	Likely Mechanisms
Fused Silica	– Flat surfaces – Easily discernible steps – Some surface craters – No thermal stress cracking	vaporization
Silicon Nitride	– Flat surfaces – Easily discernible steps – No thermal stress cracking	vaporization
Aluminum	– Surface roughness – Extremely wavy – Large pits in surface – Significant removal steps (several shots)	liquid ejection vaporization
Aluminum Oxide (Poly-crystalline and Sapphire)	– Surface roughness (wavy) – Thermal stress cracking with pits in surface – Significant removal steps (several shots)	liquid ejection thermal stress / shock vaporization
Boron Carbide and Boron	– Surface roughness (angular) – Thermal stress cracking – Rectangular pop-outs – No steps seen	thermal stress / shock
Silicon Carbide	– Surface roughness (angular) – Thermal stress cracking – Rectangular pop-outs – No steps seen	thermal stress / shock
Carbon (Amor-phous)	– Discernible steps (at highest fluences) – Some surface pitting	vaporization thermal stress / shock

E. Summary of removal depths

The primary quantitative result from these experiments was removal depths as a function of x-ray fluence. These data were obtained with the Tencor profilometer, supplemented in some cases with AFM information. The removal depths serve as the standard for the performance of any material response model. A summary of these results is plotted in Figure 1. Note that sapphire is single crystal aluminum oxide. Also, the boron carbide curve is for the best vendor's material, with other types ranging up to the boron curve. The following section discusses some of the features of individual materials.

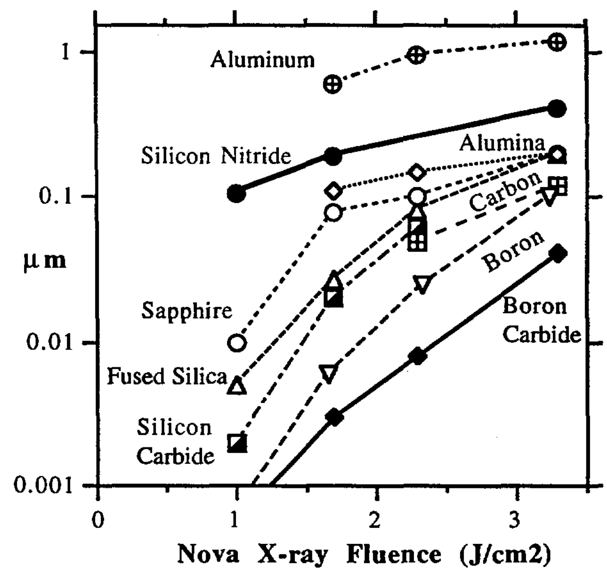

Figure 1: Summary of removal depths measured on Nova x-ray exposures. 1-2 ns pulses of 200-250 eV blackbody x rays.

IV. COMPARISON OF MODEL PREDICTIONS TO EXPERIMENTS

A. Fused Silica

The observations of the silica surfaces after exposure to x rays leads very strongly to a conclusion that vaporization is the dominant removal mechanism. The numerical model was applied using conditions matching those of the Nova experiments. The temperature profiles and vaporization behaviors were monitored for a 500-ns run. Results of the total vaporization depth as a function of x-ray fluence are plotted in Figure 2, along with the Nova data. The fit is excellent, matching both the threshold fluence and the slope at higher fluences.

It is instructive to compare the results of this new flux-limited surface vaporization model to predictions based on instantaneous-deposition energy profiles. Figure 2 also shows the predicted removal depths from two different cutoff energies as a function of x-ray fluence. Clearly neither approach produces a very good fit to the fused silica data. As discussed in the modeling section, all material down to the depth that receives this cutoff energy density is assumed to vaporize. One possible cutoff is the total vaporization (sublimation) energy, which is used in the TSUNAMI code. This provides the initial vapor conditions for the gas dynamics calculations. However, this method underestimates removal depths because it leaves behind a substantial amount of very hot material. Another choice, used in the SRI calculations, is the incipient vaporization energy, which is the energy of a liquid at some boiling temperature. By simple energy balance arguments, it is evident that this second method implies ejection of molten (or solid) material. For silica, the incipient vaporization criterion significantly overpredicts removal because vaporization is the dominant removal process.

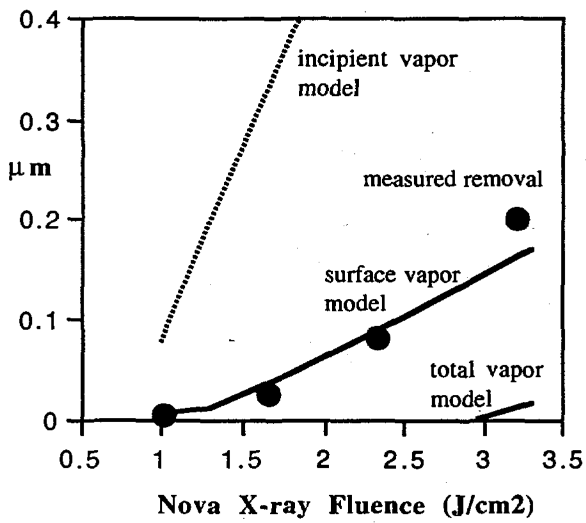

Figure 2: Fused Silica response to x rays.

B. Silicon Nitride

The response of silicon nitride looked in many ways like that of fused silica. Therefore vaporization was also judged to be the dominant removal mechanism. A complication for silicon nitride is that the vaporization process is actually a thermal decomposition of the material. At relatively low temperatures (around 3000 K), nitrogen leaves the compound as nitrogen (N_2) gas. As discussed by Tovstonog[6], at sufficiently high ablation rates the silicon is not left behind, but rather is "blown" off the surface by the large underlying pressure of nitrogen gas. The ABLATOR model incorporates the assumption that the ablated material consists of nitrogen gas mixed stoichiometrically with silicon droplets. The model results for x-ray conditions matching the Nova shots produce a very good match to the removal depth data, as shown in Figure 3.

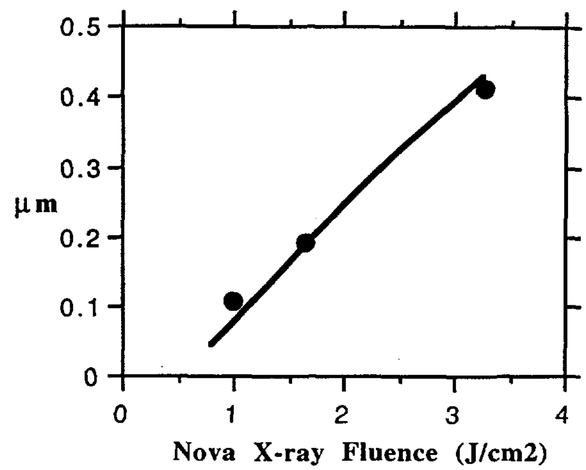

Figure 3: Silicon nitride removal measurement and surface vaporization prediction.

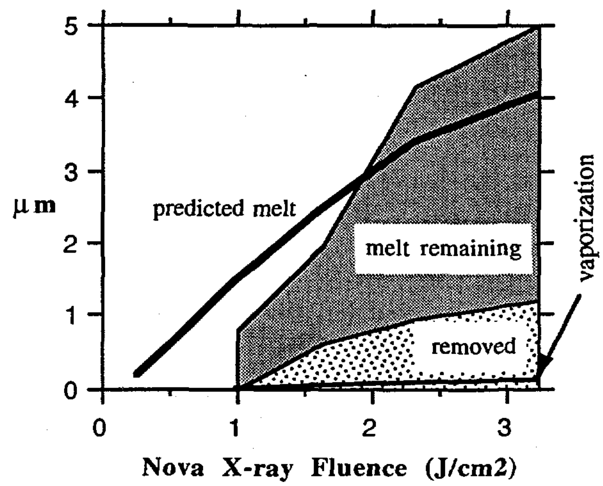

Figure 4: Melt and removal of aluminum.

C. Aluminum

Liquid ejection appears to be the dominant mechanism of material removal for aluminum. This process is consistent with the rough, wavy surface and uneven resolidified layer thickness. Aluminum has a large coefficient of thermal expansion, which could generate the forces and accelerations that would drive unstable liquid ejection. Comparisons with the model predictions of melt depth (Figure 4) show that approximately one third of the total melt layer is removed under these test conditions. In this figure, the melt remaining data is from measurements of metallographic sections in single-exposure regions where a distinct transition could be observed. The melt depth prediction (from ABLATOR) agrees well with the data. A module is being developed to estimate the growth of Rayleigh-Taylor instabilities in the liquid layer.

Vaporization was investigated as a possible contributor to the total removal depth. The ABLATOR model was applied to aluminum with the same x-ray loading used in these experiments. The vaporization was assumed to occur from a flat, 1-D interface at a rate dependent on the surface temperature and saturation pressure at that temperature. As shown in the figure, vaporization from the surface is expected to be only about 10% of the observed total removal depth. Perhaps by including the added area of the rough surfaces seen in the experiments, this estimate might be increased to 30%. At this level, vaporization could be a significant process to include in modeling, but melt ejection remains the dominant effect.

D. Aluminum Oxide

Aluminum oxide does not appear to have one single dominant damage mechanism. There is instead evidence for the contribution of several processes, that may change their relative importance depending on the particular form of alumina and the x-ray exposure conditions.

Vaporization is expected to be the lower limit for the measured removal for any material. The ABLATOR model was applied to aluminum oxide with the same x-ray loading used in these experiments. As shown in Figure 5, vaporization from the surface is expected to cause up to one third of the material removal at higher fluences. At lower fluences, the surface vaporization contribution is much less. The remaining material removal is explained by some combination of spall and liquid ejection.

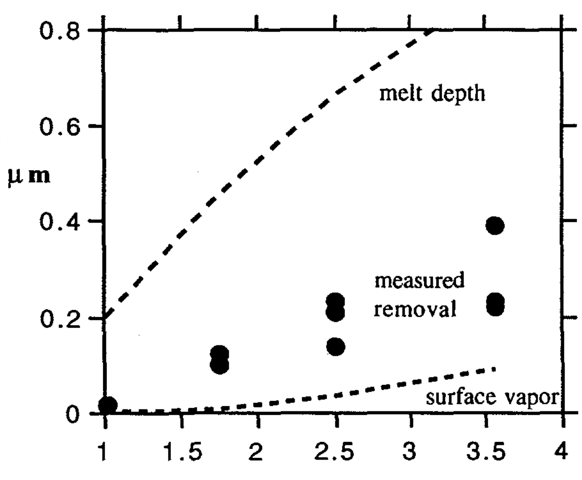

Figure 5: Measured removal depths and predicted melt depth and surface vaporization for alumina.

E. Boron Carbide and Boron

Thermal stress / shock appears to be the dominant removal mechanism for boron carbide and boron. Most samples show thermal stress cracking and all materials show surface roughening at the higher x-ray fluences. Continued exposures cause additional roughness and the appearance of angular pits in the surface. The pits seem to be locations where small sections of thermally shocked material has flaked off or was popped out by the additional thermal loading. This behavior is shown in Figure 6. The necessary models for predicting ablation depths by this mechanism, including brittle crack nucleation and growth and statistical methods for the pop-out of isolated flakes, have not been developed in the ABLATOR code.

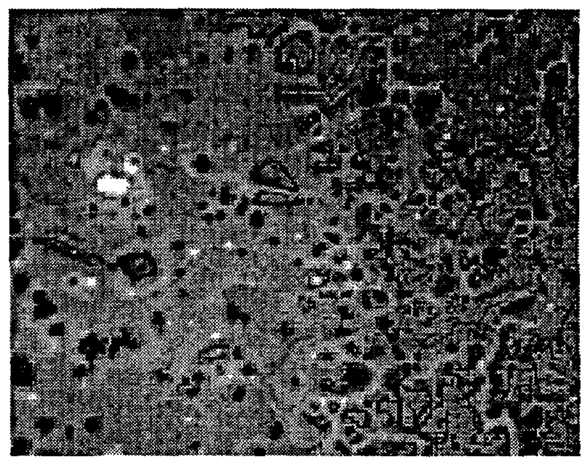

Figure 6: Boron carbide exposed to one (left) and three shots (right) at 3.5 J/cm^2.

F. Silicon Carbide

Thermal stress / shock appears to be the dominant removal mechanism. Some damage was exhibited at all fluences, with all but the lowest showing thermal stress cracking. Above 2 J/cm2 the surfaces appeared to be somewhat rounded, indicating some effects of surface melting. Profilometry showed roughening to about 2 µm peak to valley. Removal results represent estimates of pit depth and areal coverage.

G. Amorphous Carbon

Many forms of carbon are available. Our tests were conducted on pyrolytic carbon SEM stubs. These samples showed clear ablation steps at the highest fluences, indicating that vaporization is the dominant ablation mechanism. Some additional removal was caused by pitting, which may reflect surface damage from the polishing process.

V. CONCLUSIONS

The experimental results make it clear that x-ray ablation depends on several different mechanisms: vaporization, liquid splash, and thermal shock/spall. The relative importance of each of these mechanisms depends on the thermophysical properties of the material and the details of the x-ray exposure. Modeling of the vaporization process appears to be well in hand, so that at least a minimum ablation depth can be predicted for a given material. The experimental observations will continue to guide the model development efforts for the other two removal mechanisms.

ACKNOWLEDGMENTS

We wish to thank those at LLNL who performed the various post-shot analyses of these samples, in particular Evelyn Fearon, Ed Lindsey, Craig Moore, Charlotte King, and Bob Kershaw. This work was performed under the auspices of the U.S. Department of Energy by Lawrence Livermore National Laboratory under contract no. W-7405-Eng-48.

REFERENCES

1) Kipp, M.E., Lawrence, R.J., "WONDY V – A One-Dimensional Finite-Difference Wave Propagation Code", Sandia Natl Lab, SAND81-0930, June 1982.

2) Peterson, RR., MacFarlane, JJ., Moses, GA., "CONRAD – A Combined Hydrodynamics–Condensation/Vaporization Computer Code", Univ. Wisc., UWFDM-670, July 1988.

3) Chen, XM., "A Study of Thermal Hydraulic and Kinetic Phenomena in HYLIFE-II – An Inertial Confinement Fusion Reactor", PhD dissertation, UC Berkeley, Jan 1993.

4) Tokheim, RE., Seaman, L., Curran, DR., "Threats from Radiation Effects in the Proposed Nova Upgrade", SRI Intl Final Report for LLNL, Sept, 1992.

5) Kelly, R., Rothenberg, J.E., "Laser Sputtering Part III. The mechanism of the sputtering of metal at low energy densities", Nucl. Inst. & Meth, B7/8, (1985), 755-763.

6) Tovstonog, V.A., "Experimental Investigation of Thermal Decomposition of Silicon Nitride", High Temperature, 1993 May-Jun, V31 N3:535-542.